International Journal of Materials and Chemistry 2013, 3(3A): 8-15
DOI: 10.5923/s.ijmc.201303.02

Silk Fibroin/Calcium Phosphate Silicate Composites: *In vitro* Bioactivity

Lachezar Radev[1,*], Todor Gerganov[2], Hristo Georgiev[3], Antony Kolev[4], Violeta Vassileva[4], Rumiana Iankova[5], Ekaterina Cholakova[1]

[1]Department of Fundamental Chemical Technology, University of Chemical Technology and Metallurgy, Sofia, 1756, Bulgaria
[2]Department of Silicate Technology, University of Chemical Technology and Metallurgy, Sofia, 1756, Bulgaria
[3]Department of Polymer Materials, University of Chemical Technology and Metallurgy, Sofia, 1756, Bulgaria
[4]Department Leather and Textile, University of Chemical Technology and Metallurgy, Sofia, 1756, Bulgaria
[5]Department of Inorganic Chemistry, Assen Zlatarov University, Bourgas, 8000 Bulgaria

Abstract Composite materials of Silk Fibroin (SF) and Calcium Phosphate Silicate (CPS) ceramic in the $15CaO\text{-}6SiO_2\text{-}0.5P_2O_5$ system were prepared by method of mixing different percentage of component weight. The structure was characterized before and after *in vitro* test by FTIR, SEM. The concentration of Ca, Si and P after in vitro test was analysed by ICP-AES. FTIR of the composites before *in vitro* test depicts that random coil and β-sheet structures co-exist in the composites. CPS ceramic has a significant effect on the secondary structure of SF. SEM observed that CPS particles uniformly dispersed in SF matrix. FTIR of the composites after *in vitro* test revealed that carbonate containing hydroxyapatite (CO_3HA) was formed on the surface. B-type CO_3HA preferentially formed in the sample with 75 wt. % CPS ceramic. SEM proved that hydroxyapatite (HA) formed in a high level. ICP-AES showed that HA precipitation were similar for the three composites. Based of these results, it can be concluded that the incorporation of CPS ceramic powder enhanced the *in vitro* bioactivity.

Keywords Silk Fibroin, Calcium Phosphate Silicate, Composites, *In vitro* bioactivity

1. Introduction

It is well known that natural bone is a typical inorganic/organic composite comprising approximately 80 % HA and 20% collagen matrix. It is also known that the bone shows a porous structure, containing multiple levels of organization where HA crystals in nanolevel scale are embedded in collagen matrix.

The biomimetical strategy, based on the idea of mimicking natural bones composition offers great promise for the design and fabrication of biomaterials for healing bone defects. Therefore, growing interest has been focused on the integration of HA ceramic with bio-organic polymers, such as collagen[1], gelatine[2], alginate[3], polylactic acid [4], polyamide[5] and silk fibroin (SF)[6-14]. Among them SF is of practical interest due to its excellent intrinsic properties utilizable in the biotechnological and biomedical fields. It is known that SF is composed from 17 aminoacids. It has been proved to be good biocompatible material and it has been successfully used for various medical applications. X. D. Kong et al.,[6] demonstrated that silk fibres could induce HA nucleation on the surfaces proteins in simulated body fluid (SBF) solution at pH=8 at room temperature. FTIR results proved that the HA crystals are CO_3HA. On the other hand they also detected that there are strong chemical interactions between HA and SF protein. The presence of these bonds can be derived from the blue shift of amide II bond. For this reason, a co-precipitation method was often used to synthesize silk powder/HA nanocomposites[6-14]. For instance, L. Wang et al.[9] deposited HA on SF microspheres thorough the co-precipitation method. Others developed a HA/SF composite, where SF was modified with organic compound[15]. In other article, R. Kino et al.[16] reported that regenerated SF films containing calcium were coated with HA after soaking in 1.5 SBF solution for 6 hours. Y. Li et al.[17] proved that SF can induce HA deposition at 37℃ in 1.5 SBF. The effect of pH and initial Ca^{2+}-$H_2PO_4^-$ concentration on the crystal growth of HA in the presence of SF is studied by Y. Ren et al.[12]. The authors evaluate the effect of pH and initial Ca-P concentration on the products of SF mineralization. They also demonstrated that that pH=7 promotes the transition of dicalcium phosphate dihydrate (DCPD) to HA. X. Kong et al. observed that SF can accelerate the phase transmittance of amorphous calcium phosphate to the crystal hybrid between DCPD and HA[18]. L. Li et al.[19] prepared SF/Calcium Phosphate (CP) composite by adding

* Corresponding author:
l_radev@abv.bg (Lachezar Radev)
Published online at http://journal.sapub.org/ijmc

the different amount of Na_2SiO_3 to assess the effect of silicon on the HA formation in the composite. Based on the obtained results they proved that the addition of silicon could accelerate the HA crystal formation. SF/Wollastonite composite scaffolds were prepared by H. Zhu et al.[20] via freeze-drying method. The obtained results showed that the composite scaffold was *in vitro* bioactive, because it induced the formation of CO_3HA on the surface after soaking in SBF for 5 days. Four type of hybrid films were fabricated from N. Vachiraroj et al.[21]. These materials include gelatin conjugated SF, HA/SF, HA/Gelatin conjugated SF and HA/Chitosan. The synthesized films were investigated in terms of *in vitro* adhesion, proliferation and oestrogenic differentiation with preosteoblast cell lines (MC3T3-E1) and rat bone marrow derived stem cells (MC3). The authors proved that MC3T3-E1 showed higher proliferation rate.

In our previous works, we prepared some *in vitro* bioactive ceramics in the $CaO-SiO_2-P_2O_5$[22-24], and $CaO-SiO_2-P_2O_5-MgO$ systems[25] through different ways. Furthermore, we have synthesized *in vitro* bioactive composite materials in the presence of collagen[26-28] and gelatin[29, 30] with the prepared ceramics powders.

The purpose of the present article is preparing new bioactive composite by addition of SF with calcium phosphate silicate (CPS) ceramic and evaluating its bioactivity in 1.5 SBF solutions.

2. Experimental Part

CPS ceramic powder in the system $15CaO-6SiO_2-0.5P_2O_5$, as an inorganic part of the composites, has been synthesized via polystep sol-gel method. The synthesized procedure and structure evolution is documented in Ref.[23].

SF without sericin was dissolved in 9M LiBr at 60^oC for 4 hours and then dialyzed against with distilled water at room temperature for 3 days using cellulose membrane (MWCO 12000 Da) for 72 hours to remove the salts[21]. The final concentration of SF solution was 3 wt. %, which was determined in accordance with[20]. SF/CPS composites were prepared by mixing method without binding agents. Briefly, a certain amount of CPS powder was added into the SF solution under stirring for 4 hours in order to disperse the CPS particles uniformly. The obtained mixture was poured into plastic cup. The mixture was dried in the microwave oven for 10 minutes. In the present work, three kind of samples were made with the weight ratio of SF:CPS of 75:25, 50:50 and 25:75 (in wt. %), described as 75S25C, 50S50C and 25S75C.

In vitro bioactivity of the prepared composites with different weight ratio of SF and SPS were evaluated by examining the apatite formation on their surfaces in 1.5 SBF solutions. 1.5 SBF solution was prepared from reagents as follows: NaCl=11.9925 g, $NaHCO_3$=0.5295 g, KCl=0.3360 g, $K_2HPO_4.3H_2O$=0.3420 g, $MgCl_2.6H_2O$=0.4575 g, $CaCl_2.2H_2O$=0.5520 g, Na_2SO_4=0.1065 g and buffering at pH=7.4 at 36.5℃ with TRIS=9.0075 and 1M HCl in distilled water. The synthesized composite materials were immersed in 1.5 SBF at human body temperature (36.6℃) in polyethylene bottles, in static conditions for 12 days. The samples were removed from the fluid after soaking, and gently rinsed with distilled water, then dried at 37℃ for 6 hours. To prevent a homogeneous apatite formation in the solution, it is known that 1.5 SBF needed to buffered at 7.25, as it is highly supersaturated and consequently unstable[31].

The structure and the *in vitro* bioactivity of the synthesized SC composites were monitored by FTIR, ICP-AES and SEM.

FTIR transmission spectra were recordered by using a Brucker Tensor 27 Spectrometer with scanner velocity 10 kHz. Diluted pellets of KBr were prepared by mixing of ~1 mg of the samples with 300 mg KBr. Transmission spectra were recordered using MCT detector with 64 scans and 1 cm^{-1} resolution.

The samples were immersed in sealed test tubes containing 10 ml of 1.5 SBF solution for 12 days. The experiment was maintained at 37℃ in sterile polyethylene containers in static conditions. After immersion in 1.5 SBF for 12 days the samples were retrieved, gently rinsed with water, and dried at 37 ℃ for 6 hours. The ionic concentrations of Ca, P and Si of these solutions were determined by Inductively Coupled Plasma Atomic Emission Spectroscopy (ICP-AES), Iris 1000, Thermo Elemental, USA.

Morphological studies of the obtained composite materials before and after *in vitro* test for 12 days have been done by using SEM. The samples were gold-sputter coated and viewed in the secondary electron mode with a field emission gun. Scanning electron Microscope (Philips 515) operated at an accelerating voltage of 2.5 kV.

3. Results and Discussion

FTIR spectra of SF and SC composites before *in vitro* test are shown in Figure 1 in the spectrum range 2000-400 cm^{-1}.

SF proteins exists in three conformations, namely random coil, silk I (α-form) and silk II (β-sheet). The absorption band posited at 1644 cm^{-1} for SF can be ascribed to the amide I mode, associated with random coil conformation occurring in the range of 1640-1650 cm^{-1}, 1534 cm^{-1} for amide II in the random coil and the β-sheet conformations and 1240 cm^{-1} for amide III[19, 20, 31]. From the depicted in Fig. 1, a FTIR spectrum, we can assume that both random coil and β-sheets conformation are presented in the structure after microwave treatment of SF. On the other hand, three spectra of the composites with different wt. % of the SF and CPS (Fig. 1, b, c and d) show the peak shift from 1644 to 1638 cm^{-1} (for 75S25C sample), 1640 cm^{-1} (for 50S50C sample) and 1641 cm^{-1} (for 25S75C sample). In the case of 75S25C (fig. 1, b) the observed "red shift" could be ascribed to the conformational transition from random coil to β-sheet, i. e. antiparallel β-sheet conformation[32]. L. Li et al. reported

that the same result can be observed, when the composite material synthesized through biomimetic way[19]. There is another possible interpretation, from our point of view : the depicted "red shift" can be assigned to the C=O: group which may interact with Ca^{2+} from partially dissolved CPS ceramic powder in SF solution under the preparation conditions of the composites. The same results can be observed for amide II and amide III region. New bands at 714-430 cm^{-1} appear in addition to the characteristic amide I, II and III absorption bands, after preparation of the samples, were assigned to the presence of CPS ceramic[23].

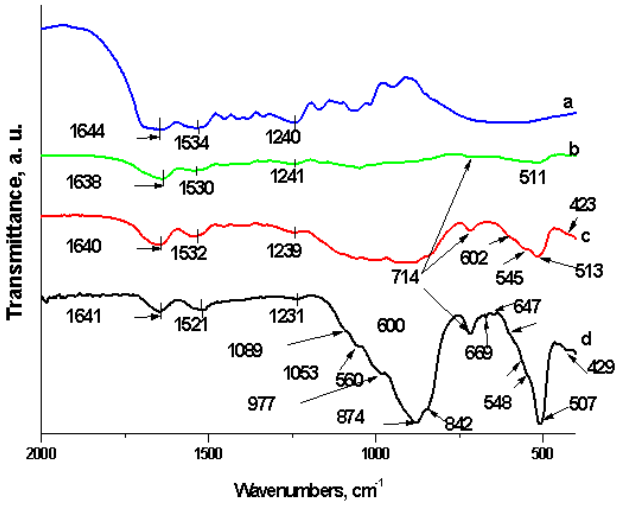

Figure 1. FTIR spectra of SF (a), 75S25C (b), 50S50C (c) and 25S75C (d) before *in vitro* test

From the presented FTIR data we can see that when SF solutions was mixed with CPS ceramic powder and undergo microwave treatment, further conformational changes may occur, with a further transition of random coils to a more stable, antiparallel β-sheet conformation throughout intermediate forms, such as β-turns and β-blends.

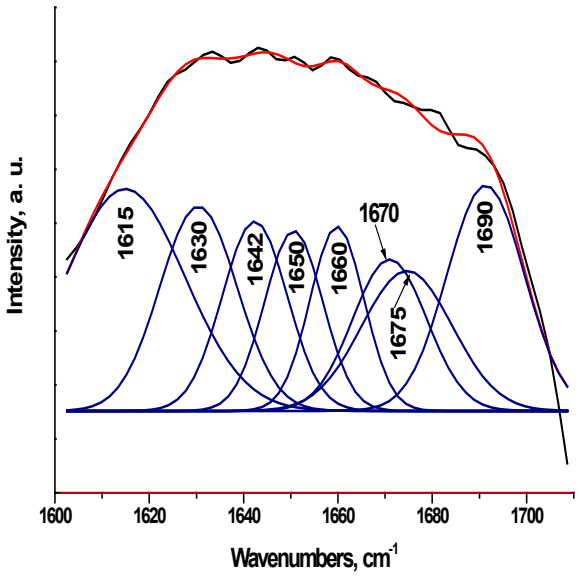

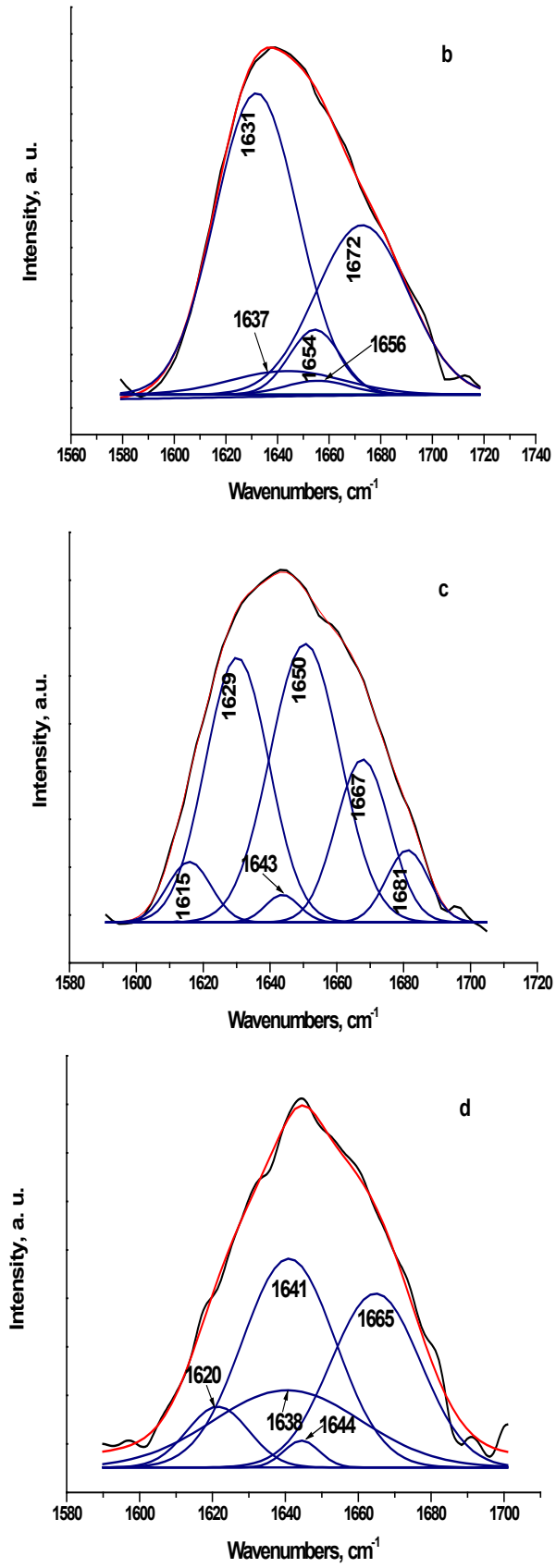

Figure 2. Curve-fitting results of the FTIR spectra in the amide I region for the SF (a), 75S25C (b), 50S50C (c), and 25S75C (d)

FTIR spectra of SF and SF/CPS composites were examined more carefully in the amide I region. The amide I spectral region was resolved into 3 of 4 main components for SF and for composites, assuming a Gaussian behavior for each individual process. The curve-fitting results are shown in Figure 2 and Table 1.

Table 1. Curve-fitting results of "amide I" regions In FTIR spectra of the SF and SF/CPS composites

Sample	Wavenumbers, cm^{-1}	Peak area, %	Type of structure
SF	1615	23	β-structure
	1630	14	β-structure
	1642	11	Random coil
	1650	9	Random coil
	1660	9	β-turns and blends
	1670	10	β-turns and blends
	1675	11	β-structure
	1690	15	β-turns and blends
75S25C	1631	59	β-structure
	1637	6	β-structure
	1654	8	β-structure
	1656	2	β-turns and blends
	1672	37	β-structure
50S50C	1615	8	β-structure
	1643	3	Random coil
	1650	61	Random coil
	1667	27	β-turns and blends
	1681	9	β-turns and blends
25S75C	1620	8	β-structure
	1638	2	β-structure
	1641	41	Random coil
	1644	24	Random coil
	1665	33	β-turns and blends

We can see from the presented in Figure 2 and Table 1 curve-fitting data, that in the sample with 25 wt. % CPS ceramic powder, the β-structure fraction significantly increased in parallel with pure SF. Furthermore, the fractions of β-structure significantly decreased, but the random coil fraction slightly increased, compared with pure SF, with increasing of CPS ceramic powder to 50 and 75 wt. %. Finally, the fraction of β-turns and blends does not significantly change comparing to SF.

We can conclude that significant changes in the percentage of β-structure, random coil and β-turns and blends are observed among the pure SF and SF/CPS composites, i. e. the addition of different weight of CPS ceramic has a significant effect on the secondary structure of SF. These observations are needed for future investigations.

SEM micrographs of the prepared composites with different weight ratio of the two components are shown in Figure 3.

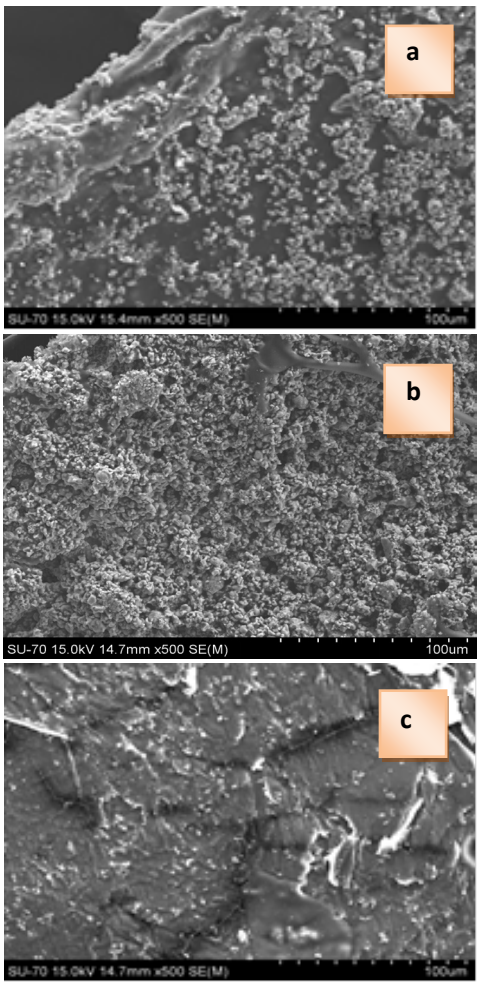

Figure 3. SEM of 25S75C (a), 50S50C (b) and 75S25C (c) before *in vitro* test in 1.5 SBF

SEM micrographs of the synthesized composites before soaking in 1.5 SBF for various periods of time show that the original materials present textural differences. While 25S75C (Fig. 3, a) and 75S25C (Fig. 3, c) show a heterogeneous distribution of a ceramic powder over fibroin, 50S50C (Fig. 3, b) presents a more homogeneous surface when the organic and inorganic parts of the composite are equal. The fiber structure of fibroin was visibly recognized in the 25S75C and 50S50C samples (Fig. 3 a and b). When the quantity of fibroin increased to the 75 wt. % (Fig. 6, c) the SEM image shows the different textural future. It can be seen, the prepared sample consisting large individual fibroin lamella with a ceramic powder on the surface. The observed lamella in the 75S25C sample is a function of water residence time in the process of microwave drying of the prepared composite material. From general point of view, the synthesized fibroin-calcium phosphate silicate composites without any previous treatment, dried in microwave oven (Fig. 3, a-c) exhibit a smoother aggregate surface. This

smooth surface is explained by the migration of fine ceramic particles and their coalescence on the fibroin surface, driven by different mechanisms of drying. As it can be read in E. Pecoraro et al.[33], the solvent activation energy (in our case water) can cause aggregate collapse which can give polycondensation ceramic particles and smoother surface of the prepared organic/inorganic composites.

The FTIR spectra of the synthesized SF/CPS composites after in vitro test in 1.5 SBF for 12 days are presented in Figure 4

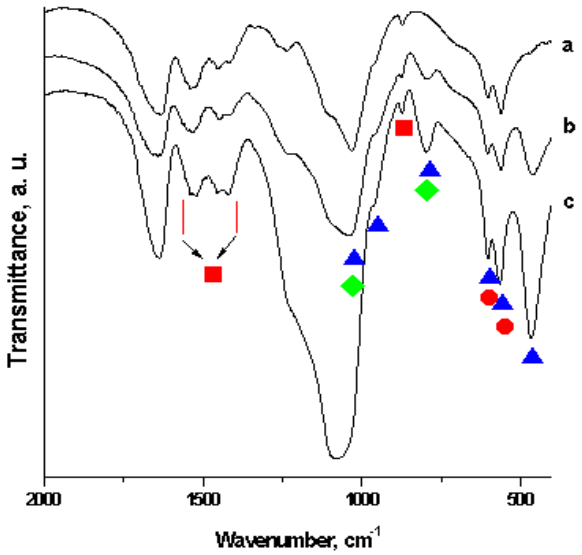

Figure 4. FTIR spectra of the SF/CPS composites: 75S25C (a), 50S50C (b) and 25S75C (c) after in vitro test in 1.5 SBF for 12 days in static conditions

The very important vibration of the PO_4^{3-} bands in the depicted FTIR spectra (▲) could be distinguished in the three main regions: (i) the peaks with very small intensity, centered at 1040 cm^{-1} (Fig. 4, b and c) are associated with asymmetric stretch vibration[34]. The presence of these peaks related with stretching vibrations of PO_4^{3-} in apatite crystalline phases[35], (ii) a weak band, posited at ~960 cm^{-1} (Fig.4 a, b and c) corresponding to the symmetric stretching[34], and (iii) the well resolved triplet at 600, 560 and 470 cm^{-1} could be ascribed to the asymmetric modes. On the other hand, the peak at ~1040 cm^{-1} and the peaks at ~796 cm^{-1} (Fig. 4 b and c) could be ascribed due to the both of the PO_4^{3-} and Si-O-Si (♦) band[36]. Furthermore, the peaks at 600 and 560 cm^{-1} are assigned to O-Si-O (●) vibration[37]. In addition the bands in the region 1560-1400 cm^{-1} and the band at ~875 cm^{-1} could be assigned to the presence of CO_3^{2-} (■) vibrations[22, 23, 25, 27-30].

More detailed information about the type of substitution in CO_3HA, formed on the surface of the SF/CPS samples, after 12 days of immersion in 1.5 SBF, was given by curve-fitting in the region 1400-1600 cm^{-1} (Figure 5)

From the depicted in Figure 5 results, it can be seen that the bands, posited at 1409, 1417, 1446, 1452, 1454, 1457, 1470, 1521, 1523, 1526, 1538 and 1539 cm^{-1} could be ascribed to the presence of B-type CO_3HA, i. e. part of PO_4^{3-} replaced by CO_3^{2-}[13, 28, 38-40]. The bands, centered at 1500, 1508, 1514, 1516, 1550 and 1570 cm^{-1} could be assigned to A-type substitution in which $CO_3^{2-} \rightarrow OH^-$[38, 41, 42]. Furthermore, there are some bands, posited at 1422, 1436 and 1547 cm^{-1}. They could be denoted as indicative bands for A/B-type CO_3HA in accordance with[43].

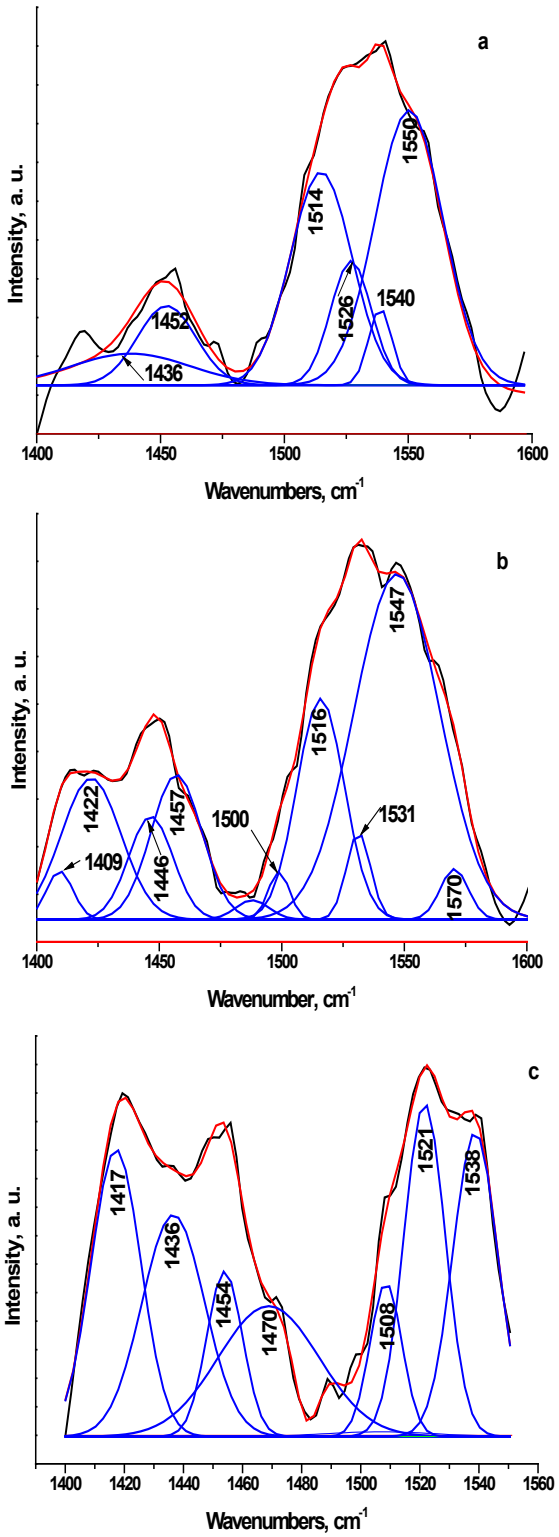

Figure 5. Curve-fitting spectra of the type of CO_3HA, formed on the surface of SF/CPS composites: 75S25C (a), 50S50C (b) and 25S75C (c) after in vitro test in 1.5 SBF for 12 days in static conditions

The curve-fitting results including peak area (%) are shown in Table 2.

Table 2. Curve-fitting results of CO_3^{2-} regions in the SF/CPS composites after in vitro test for 12 days in 1.5 SBF solutions in static condition

Sample	Wavenumbers, cm^{-1}	Peak area, %	Type of CO_3HA
75S25C	1438	9	A/B
	1452	11	B
	1514	30	A
	1526	12	B
	1538	4	B
	1550	43	A
50S50C	1409	2	B
	1422	13	A/B
	1446	7	B
	1457	11	B
	1500	2	A
	1516	16	A
	1531	3	B
	1547	45	A
	1570	2	A
25S75C	1417	18	B
	1436	16	A/B
	1454	7	B
	1470	18	B
	1508	11	A
	1523	17	B
	1539	14	B

We can conclude, from the depicted in Table 2 results, that B-type CO_3HA (bioapatite) was preferentially observed, when CPS ceramics was 75 wt. % into the composite.

Figure 6 shows SEM images of the surfaces for studied composite materials with different weight ratio of SF and CPS, after soaking in 1.5 SBF solution for 12 days in static conditions

It is observed, from depicted SEM results, that the surface of the immersed samples fully covered from the particles with different morphology. The observed spherical particles seem have crackles at the beginning, but actually they have not. We can see, from the presented at Fig. 6 a, b and c SEM data, that the big spherical particles and small spheres with diameter up to ~2 µm are composed.

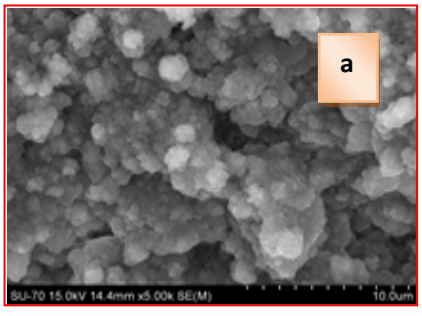

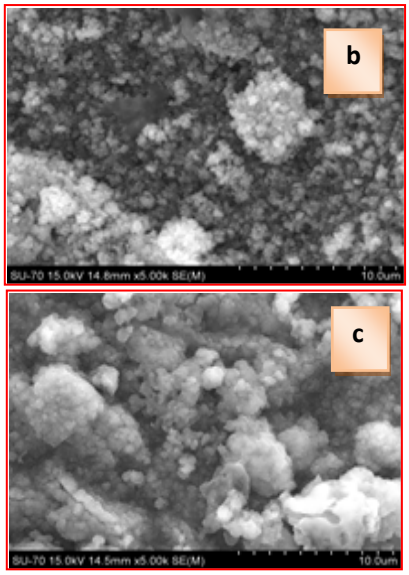

Figure 6. SEM images for 75S25C (a), 50S50C (b) and 25S75C (c) after soaking in 1.5 SBF solution for 12 days

Figure 7 presents The ICP-AES data for the evaluation of the ionic concentration of Ca, Si and P in the 1.5 SBF solution after soaking of the SF/CPS composites for 12 days.

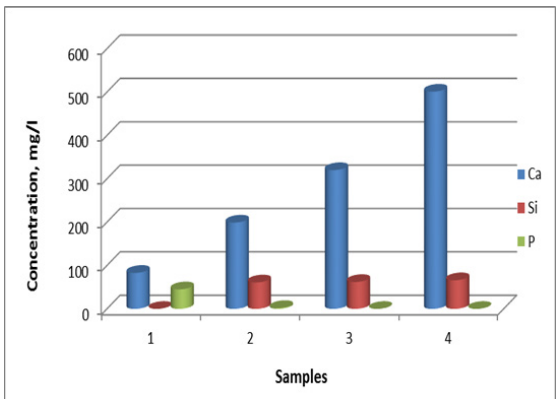

Figure 7. Changes in Ca, Si and P concentration for the 1.5 SBF solution (sample 1) and SF/CPS composites: *75S25C (sample 2), 50S50C (sample 3) and 25S75C (sample 4) after* in vitro *test in 1.5 SBF for 12 days*

It can be seen from the presented Fig. 7 that the Ca concentration for the samples 2-4 slightly increased, compared with the Ca concentration into the initial 1.5 SBF solution. The concentrations of Ca are in accordance with the weight ratio of the CPS ceramic powder in the prepared SF/CPS samples. We could see from the presented Fig.7, that the Si content in 1.5 SBF solutions increased up to 66 mg/l (sample 4). In accordance to our preliminary data[28], we can conclude that silicon containing CO_3HA (Si-CO_3HA) may be formed on the surface of the immersed samples for 12 days. Finally, the P concentration slightly decreased from 45 mg/l for the 1.5 SBF solution (sample 1) to 2 mg/l (sample 2) and 0 mg/l (samples 3 and 4). The obtained ICP-OES data indicates that the outset of HA precipitation is similar to the three composites, although the stronger one better resolved FTIR ν_2 PO_4^{3-} vibrations, posited at 560-567 cm^{-1}. The presence of these bands suggests that the HA layer possesses superior structural order on the composites after soaking.

The presented ICP-AES data is in a good agreement with FTIR and SEM analysis of the immersed samples.

4. Conclusions

The purposes of the presented article were to prepare and to evaluate *in vitro* bioactivity of composites between SF and CPS ceramic powder. The SF, denoted by S, was mixed with CPS ceramic powder, denoted by C, to prepare 75S25C, 50S50C and 25S75C composites. The obtained mixtures were treated in microwave oven to evaporate the water solvent. After drying, the prepared composites were soaked in 1.5 SBF for 12 days in static conditions to evaluate their *in vitro* bioactivity. The obtained composites were characterized by FTIR and SEM. The ionic concentration of Ca, Si and P were examined by ICP-OES technique.

FTIR data of the composites before *in vitro* test proved that the "red shift" of amide II band becomes larger in comparison to amide I and II. These findings suggest that the chemical interaction exists between SF and CPS ceramic powder. After soaking of the synthesized samples in 1.5 SBF for 12 days FTIR results proved that B-, A- and A/B-type CO_3HA are deposited on the surface. ICP-AES measurements have shown that the rates of Ca realize are ordered as follows: 25S75C>50S50C>75S25C. For the three samples, the Si concentration increased and P concentration decreased after immersion. Based on these results we suppose that Si-CO_3HA may be formed on the composite surface. SEM of the immersed samples proved that there is high concentration of HA phase on the surface.

REFERENCES

[1] S. Liao, M. Ngiam, F. Watari, S.Ramakrishna, C. K. Chan. *Systematic fabrication of nano-carbonated hydroxyapatite/collagen composites for biomimetic bone grafts*, Bioinspiration & Biomimetics, 2[3], 37-42, 2007.

[2] X. Liu, L. A. Smith, J. Hu, P. X. Ma. *Biomimetic nanofibrous gelatin/apatite composite scaffolds for bone tissue engineering.* Biomaterials, 30[12], 2252–8, 2009.

[3] M. Lee, W. Li, R. K. Siu, J. Whang, X. Zhang, C. Soo, et al. *Biomimetic apatite-coated alginate/chitosan microparticles as osteogenic protein carriers*. Biomaterials, 30[30], 6094–101, 2009.

[4] X. Cai, H. Tong, X. Shen, W. Chen, J. Yan, J. Hua, *Preparation and characterization of homogeneous chitosan–polylactic acid/hydroxyapatite nanocomposite for bone tissue engineering and evaluation of its mechanical properties*, Acta Biomaterialia, 5[7], 2693-703, 2009.

[5] X. Zhang , Y. Li, G. Lv, Y. Zuo, Y. Mu, *Thermal and crystallization studies of nano-hydroxyapatite reinforced polyamide 66 biocomposites,* Polymer Degradation and Stability, 91[5], 1202-7, 2006.

[6] Kong XD, F. Z. Cui, X. M. Wang, M. Zhang, W. Zhang, *Silk fibroin regulated mineralization of hydroxyapatite nanocrystals,* Journal of Crystal Growth, 270[1-2], 197-202, 2004.

[7] R. Nemoto, L. Wang, M. Aoshima, M. Senna, T. Ikoma, J. Tanaka, *Increasing the Crystallinity of Hydroxyapatite Nanoparticles in Composites Containing Bioaffinitive Organic Polymers by Mechanical Stressing*, Journal of the American Ceramic Society, 87[6], 1014-7, 2004.

[8] R. Nemoto, S. Nakamura, T. Isobe, M. Senna, *Direct Synthesis of Hydroxyapatite-Silk Fibroin Nano-Composite Sol via a Mechanochemical Route*, Journal of Sol-Gel Science and Technology, 21[1-2], 7-12, 2001.

[9] L. Wang, R. Nemoto, M. Senna, *Effects of alkali pretreatment of silk fibroin on microstructure and properties of hydroxyapatite-silk fibroin nanocomposite*, Journal of Materials Science: Materials in Medicine, 15[3], 261-5, 2004.

[10] Ch. Du, J. Jin, Y. Lia, X. Kong, K. Weic, J. Yao. *Novel silk fibroin/hydroxyapatite composite films: Structure and properties*. Materials Science and Engineering: C, 29[1], 62-8, 2009.

[11] R. Nemoto, L. Wang, T. Ikoma, J. Tanaka, M. Senna. *Preferential Alignment of Hydroxyapatite Crystallites in Nanocomposites with Chemically Disintegrated Silk Fibroin*. Journal of Nanoparticle Research, 6[2], 259-65, 2004.

[12] Y. Ren, X. Sun, F. Ciu, *Effects of pH and initial* Ca^{2+}-H_2PO_4-*concentration on fibroin mineralization,* Frontiers of Materials Science, 1[3], 258-62, 2007.

[13] Ch. Fan, J. Li, G. Xu, H. He, X. Ye, Y. Chen, et al., *Facile fabrication of nano-hydroxyapatite/silk fibroin composite via a simplified coprecipitation route,* Journal of Materials Science: Materials in Medicine, 45[21], 5814-9, 2010

[14] L. Wang, Ch. Li, M. Senna. "High-affinity integration of hydroxyapatite nanoparticles with chemically modified silk fibroin". Journal of Nanoparticle Research 2007;9[5]:919-29.

[15] T. Furuzono, K Ishihara, N Nakabayashi, Y Tamada, *Chemical modification of silk fibroin with 2-methacryloyloxy ethyl phosphorylcholine. II. Graft-polymerization onto fabric through 2-methacryloyloxyethyl isocyanate and interaction between fabric and platelets*, Biomaterials, 21[4], 327-33, 2000.

[16] R. Kino, T. Ikoma, A. Monkawa, S. Yunoki, M. Munekata, J. Tanaka, et al., *Deposition of bone-like apatite on modified silk fibroin films from simulated body fluid*, Journal of Applied Polymer Science, 99[5], 2822-283, 2006.

[17] Y. Li, Y. Cai, X. Kong, J.Yao, *Anisotropic growth of hydroxyapatite on the silk fibroin films*, Applied Surface Science, 255[5], 11681-5, 2008.

[18] X. Kong, X. Sun, F. Cui, Ch. Ma. *Effect of solute concentration on fibroin regulated biomineralization of calcium phosphate,* Materials Science and Engineering: C, 28[4], 639-43, 2006.

[19] L. Li, K-M Wei, F. Lin, X-D Kong, J-M. Yao. *Effect of silicon on the formation of silk fibroin/calcium phosphate composite*, Journal of Materials Science: Materials in Medicine, 19[2], 577-82. 2008

[20] H. Zhu, J. Shen, X. Feng, H. Zhang, Y. Guo, J. Chen, *Fabrication and characterization of bioactive silk*

fibroin/wollastonite composite scaffolds, Materials Science and Engineering: C, 30[1], 132-40, 2010.

[21] N. Vachiraroj, J. Ratanavaraporn, S. Damrongsakkul, R. Pichyangkura, T. Banaprasert, S. Kanokpanont, *A comparison of Thai silk fibroin-based and chitosan-based materials on in vitro biocompatibility for bone substitutes*, International Journal of Biological Macromolecules, 45:470-7, 2009.

[22] L. Radev, V. Hristov, I. Michailova, B. Samuneva, *Sol-gel bioactive glass-ceramics Part I: Calcium phosphate silicate/wollastonite glass-ceramics*, Central European Journal of Chemistry, 7[3]:317-2, 2009.

[23] L. Radev, V. Hristov, I. Michailova, M. Helena V. Fernandes, I. Miranda M. Salvado, *In vitro bioactivity of biphasic calcium phosphate silicate glassceramic in CaO-SiO_2-P_2O_5 system*, Processing and Application of Ceramics, 4[1], 15-24, 2010.

[24] N. Y. Mostafa, A. A. Shaltout, L. Radev, H. M. Hassan, *In vitro surface biocompatibility of high-content silicon-substituted calcium phosphate ceramics*, Central European Journal of Chemistry, 11[2], 140-50, 2013

[25] L. Radev, V. Hristov, I. Michailova, B. Samuneva, *Sol-gel bioactive glass-ceramics Part II: Glass-ceramics in the CaO-SiO_2-P_2O_5-MgO system*, Central European Journal of Chemistry, 7[3]: 322-7, 2009

[26] V. Hristov, L. Radev, B. Samuneva, G. Apostolov, *Organic / inorganic bioactive materials Part I: Synthesis, structure and in vitro assessment of collagen/silicocarnotite biocoatings*, Central European Journal of Chemistry, 7[4], 702-10, 2009

[27] L. Radev, V. Hristov, B. Samuneva, D. Ivanova. *Organic/Inorganic bioactive materials Part II: in vitro bioactivity of Collagen-Calcium Phosphate Silicate/Wollastonite hybrids*, Central European Journal of Chemistry, 7[4], 711-20, 2009.

[28] L. Radev, N. Y. Mostafa, I. Michailova, I. M. M. Salvado, M. H. V. Fernandes, *In VitroBioactivity of Collagen/Calcium Phosphate Silicate Composites, Cross-Linked with Chondroitin Sulfate,* International Journal of Materials and Chemistry, 2[1], 1-9, 2012.

[29] L. Radev, M. Helena V. Fernandes, I. Miranda Salvado, D. Kovacheva, *Organic/Inorganic bioactive materials Part III: in vitro bioactivity of gelatin/silicocarnotite hybrids*, Central European Journal of Chemistry, 7[4], 721-30, 2009

[30] L. Radev, V. Hristov, M. Helena V. Fernandes, I. M. Miranda Salvado, *Organic/inorganic bioactive materials part IV: In vitro assessment of bioactivity of gelatin-calcium phosphate silicate/wollastonite hybrids*, Central European Journal of Chemistry, 8[2], 278-84, 2010.

[31] L. Guo, M. Huang, X. Zhang, *Effects of sintering temperature on structure of hydroxyapatite studied with Rietveld method*, Journal of Materials Science: Materials in Medicine, 14[9], 817-22, 2003

[32] S. S. Silva, D. Maniglio, A. Motta, J. F. Mano, R. L. Reis, C. Migliaresi, *Genipin-Modified Silk-Fibroin Nanometric Nets*, Macromolecular Bioscience, 8[8], 766-74, 2008.

[33] E. Pecoraro, M. R. Davolos, M. Jafelicci, Silica Morphology *Characterized by SEM. The Effects of the Solvent Treatment and the Drying Process*, Journal of the Brazilian Chemical Society,6[4], 337-41, 1995.

[34] S. R. Federman, V. C. Costa, D. C. Vasconcelos, W. L. Vasconcelos, *Sol-gel SiO_2-CaO-P_2O_5 biofilm with surface engineered for medical application*, Materials Research, 10,177-812007.

[35] D. Luna-Zaragoza, E. T. Romero-Guzmán, L. R. Reyes-Gutiérrez, *Surface and Physicochemical Characterization of Phosphates Vivianite, $Fe_2(PO_4)_3$ and Hydroxyapatite, $Ca_5(PO_4)_3OH$*, Journal of Minerals & Materials Characterization & Engineering, 8[8], 591-609, 2009.

[36] M.R. Majhi, R. Pyare, S.P.Singh, *Studies on preparation and characterizations of CaO-Na_2O-SiO_2-P_2O_5 bioglass ceramics substituted with Li_2O, K_2O, ZnO, MgO, and B_2O_3*, International Journal of Scientific & Engineering Research, 2[9], 1-9, 2011.

[37] N. Y. Mostafa, H. M. Hassan, O. Elkader, *Preparation and Characterization of Na^+, SiO_4^{4-}, and CO_3^{2-} Co-Substituted Hydroxyapatite*, Journal of the American Ceramic Society, 94[5] 1584-90, 2011.

[38] P. Regnier, A. C. Lasaga, R. A. Berner, O. H. Han, K. W. Zilm, Mechanism of CO_3^{2-} substitution in carbonate-fluorapatite: Evidence from FTIR spectroscopy,13 C NMR and quantum mechanicalc calculations, American Mineralogist, 78, 809-18, 1994.

[39] R. Santos, R. Clayton, *The carbonate content in high-temperature apatite: An analytical method applied to apatite from the Jacupiranga alkaline complex*, American Mineralogist, 80, 336-44, 1995.

[40] M. Fleet, Infrared spectra of carbonate apatites: ν_2-Region bands, Biomaterials, 30[8], 1473-81, 2009.

[41] M. E. Fleet, X. Liu, *Location of type B carbonate ion in type A-B carbonate apatite synthesized at high pressure*, Journal of Solid State Chemistry, 177[9], 3174-82, 2004.

[42] J. Kolmas, A. Jaklewicz, A. Zima, M. Bućko, Z. Paszkiewicz, J. Lis, et al., *Incorporation of carbonate and magnesium ions into synthetic hydroxyapatite: The effect on physicochemical properties*, Journal of Molecular Structure, 987[1-3], 40-50, 2011.

[43] J. P. Lafon, E. Champion, D. Barnache-Assolant, *Processing of AB-type carbonated hydroxyapatite $Ca_{10-x}(PO_4)_{6-x}(CO_3)_x(OH)_{2-x-2y}(CO_3)_y$ ceramics with controlled composition*, Journal of the European Ceramic Society, 28[1], 139-47, 2008.